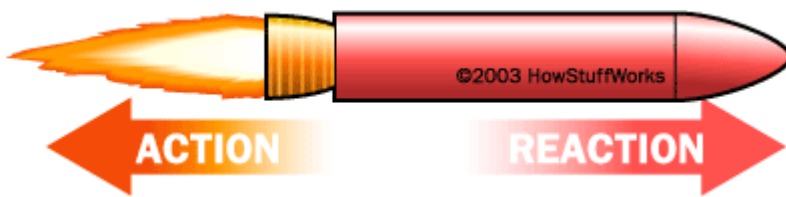


How a Rocket Engine Works

A rocket engine is not like a conventional engine. A conventional engine ignites fuel which then pushes on some pistons, and it turns a crank. Therefore, it uses rotational energy to turn the wheels of the vehicle. Electric motors also use rotational energy to turn fans, and spin disks. A rocket engine does not use rotational energy to run. They are reaction engines. The principle of it is that the fuel contained within the body of the rocket goes through a chemical reaction as it comes out of the end of the rocket. This reaction then causes thrust and propels the rocket forward. This is an example of one of Sir Isaac Newton's fundamental laws. "For every action, there is an equal and opposite reaction" (How Rocket Engines Work.)



This is a representation of Newton's law.
(<http://www.howstuffworks.com/rocket.htm/>)

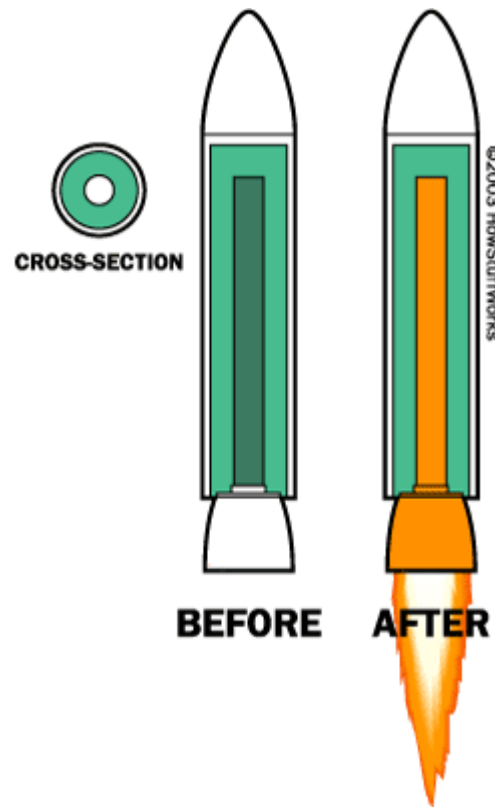


This is a picture of a space shuttle rocket engine during a test burn. Notice the blue flame of the fuel igniting. This cause thrust, and pushes the rocket in the opposite direction.
(<http://www.howstuffworks.com/rocket.htm/>)

The strength of a rocket is measured in pounds of thrust. A pound of thrust is the amount of force required to keep a one pound object stationary against gravity (How Rocket Engines Work.) In order to generate this thrust, rockets burn one of two types of fuel, solid fuel or liquid fuel. Because of this fact, rockets are often classified by the type of fuel that they burn.

Solid Fuel Rockets

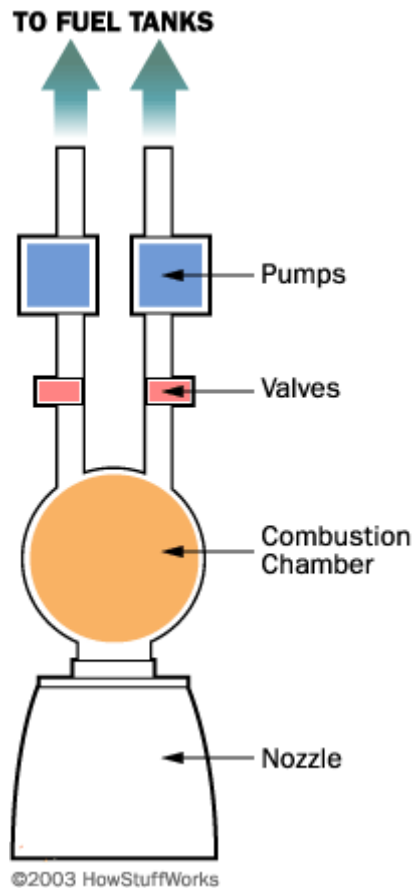
Solid fuel rockets are the first rockets to be recorded in history. They were first invented in ancient China, and have been used ever since (How Rocket Engines Work.) The chemical make up of a solid rocket fuel is very similar to the chemical makeup of gunpowder. However, the exact chemical make up is not the same. To make a rocket work, a fast burning nonexclusive fuel is needed. Gunpowder explodes, making it unusable. So the chemical composition was altered to make it burn fast, but not explode. One of the biggest problems with solid fuel rocket engines is that once started, the reaction cannot be stopped or restarted. This makes them considered uncontrollable. Therefore, solid fuel rockets are more widely used for missiles, or as booster rockets.



This is a diagram of how A solid fuel rocket engine looks before and after ignition. The solid fuel is in dark green, and then in orange as it is ignited to propel the rocket. (<http://www.howstuffworks.com/rocket.htm>)

Liquid Fuel Rockets

The first liquid fuel rocket was produced by Robert Goddard in 1926 (How Rocket Engines Work.) The idea of liquid fueled rocket is easy to grasp. A fuel and an oxidizer ,in Goddards case he used gasoline and liquid oxygen, are pumped into a combustion chamber. A reaction takes place, and it expands propelling the rocket forward. The expanding gas is then forced through a nozzle that makes them accelerate to a higher velocity (How Rocket Engines Work.)



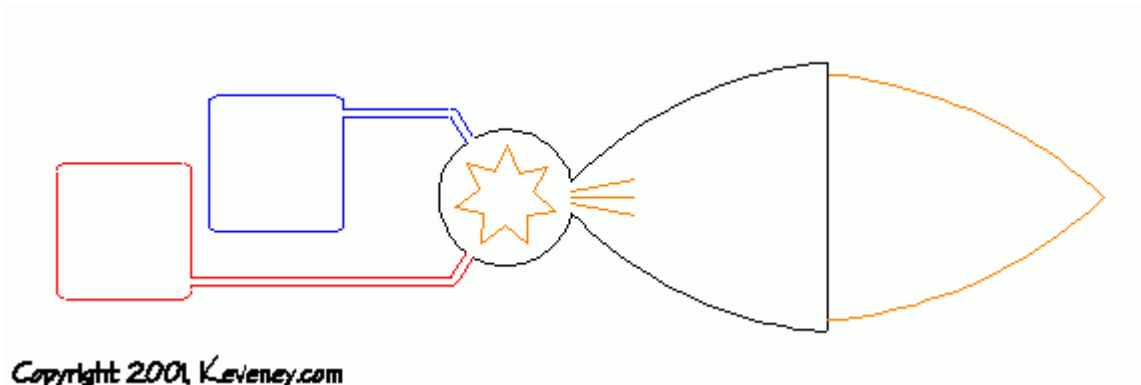
This diagram is a basic model of how a liquid fuel rocket engine works. It is easy to see that a liquid fueled rocket is much more complex than a solid fueled one. (<http://www.howstuffworks.com/rocket.htm>)

Jet Propulsion

I've grudgingly included this section by popular request. Rocket and turbojet engines are fabulous technological achievements--But they're so simple the animations are boring!

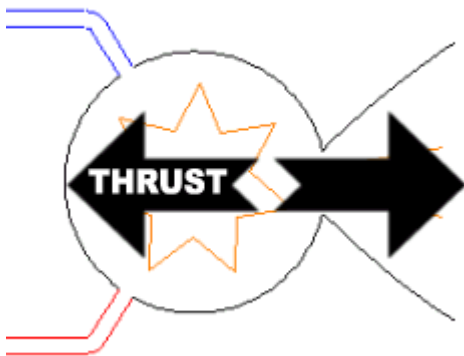
...At least I think so. You be the judge!

Rocket



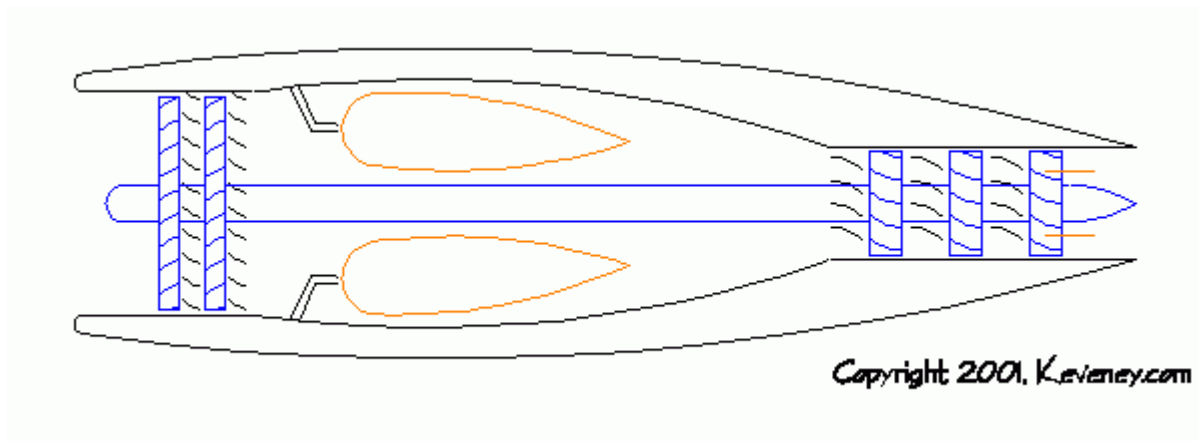
The rocket engine is the simplest of this family, so I'll start with it.

In order to work in outer space, rocket engines must carry their own supply of oxygen as well as fuel. The mixture is injected into the combustion chamber where it burns continuously. The high-pressure gas escapes through the nozzle, causing thrust in the opposite direction.



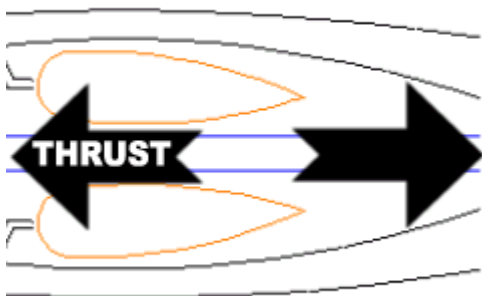
To illustrate the principle yourself, inflate a toy balloon and release it (without tying it off!). ...rocket propulsion at its simplest.

Turbojet



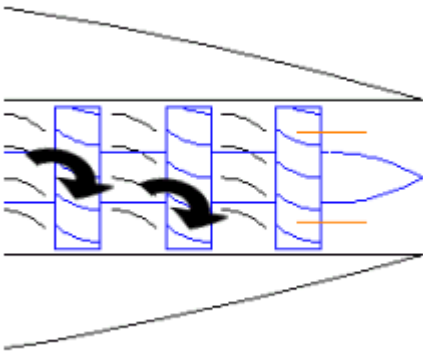
The turbojet employs the same principle as the rocket. It burns oxygen from the atmosphere instead of carrying a supply along.

Notice the similarities: Fuel continuously burns inside a combustion chamber just like the rocket. The expanding gasses escape out the nozzle generating thrust in the opposite direction.

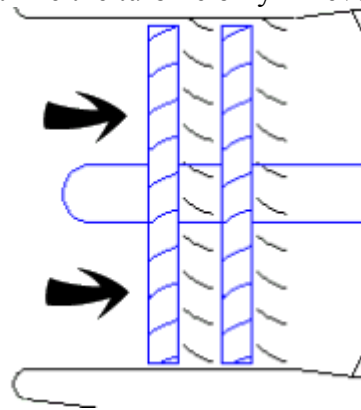


Now the differences: On its way out the nozzle, *some* of the gas pressure is used to drive a *turbine*. A turbine is a series of *rotors* or fans connected to a single

shaft. Between each pair of rotors is a *stator* -- something like a stationary fan. The stators realign the gas flow to most effectively direct it toward the blades of the next rotor.



At the front of the engine, the turbine shaft drives a *compressor*. The compressor works a lot like the turbine only in reverse. Its purpose is to draw air

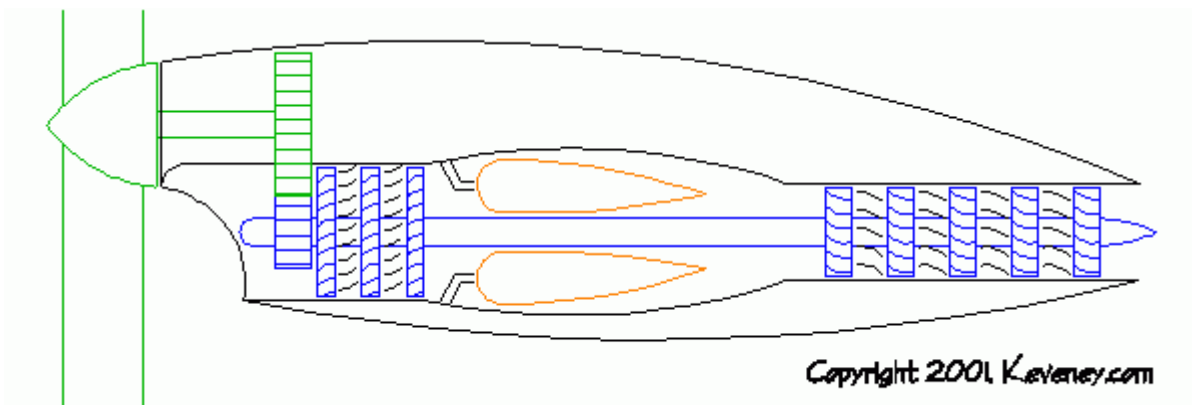


into the engine and pressurize it.

Turbojet engines are most

efficient at high altitudes, where the thin air renders propellers almost useless.

Turboprop

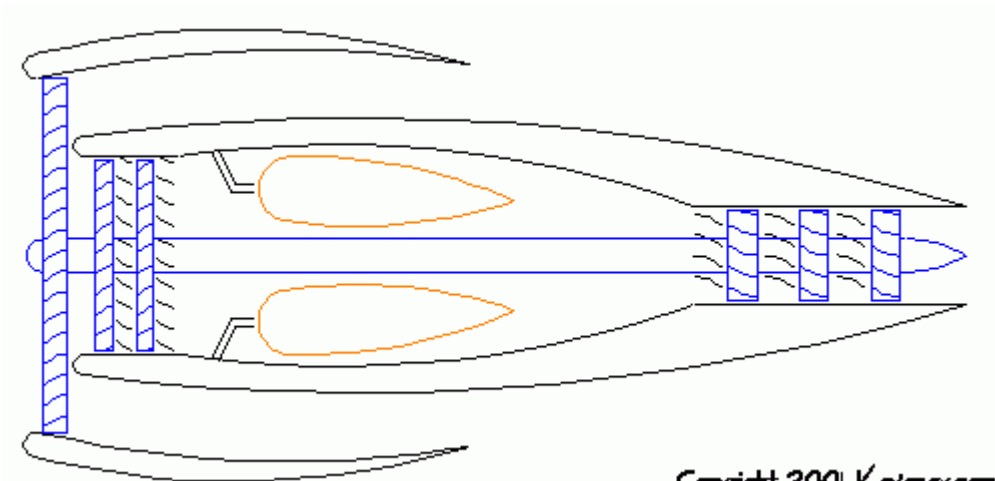


The turboprop is similar to the turbojet, except that *most* of the nozzle gas pressure drives the turbine shaft -- by the time the gas gets past the turbine, there's very little pressure left to create thrust.

Instead, the shaft is geared to a propeller which creates the majority of the thrust. 'Jet' helicopters work the same way, except that their engines are connected to the main rotor shaft instead of a propeller.

Turboprops are more fuel efficient than turbojets at low altitudes, where the thicker air gives a propeller a lot more 'traction.' This makes them popular on planes used for short flights, where the time spent at low altitudes represents a greater percentage of the overall flight time.

Turbofan



The turbofan is something like a compromise between a pure turbojet and a turboprop. It works like the turbojet, except that the turbine shaft also drives an external fan, usually located at the front of the engine.

The fan has more blades than a propeller and spins much faster. It also features a shroud around its perimeter, which helps to capture and focus the air flowing through it. These features enable the fan to generate some thrust at high altitudes, where a propeller would be ineffective.

Much of the thrust still comes from the exhaust jet, but the addition of the fan makes the engine more fuel efficient than a pure turbojet. Most modern jetliners now feature turbofan engines.

As you can see all of these engines are conceptually very simple, and have very few moving parts, making them extremely reliable. They also have an excellent power-to-weight ratio, which is partly why they're so popular in aircraft.

Like most of my illustrations, these are extremely simplified. Turbine engines often employ more than one shaft and have other more complex features that I really don't understand and, frankly, don't care to investigate further.

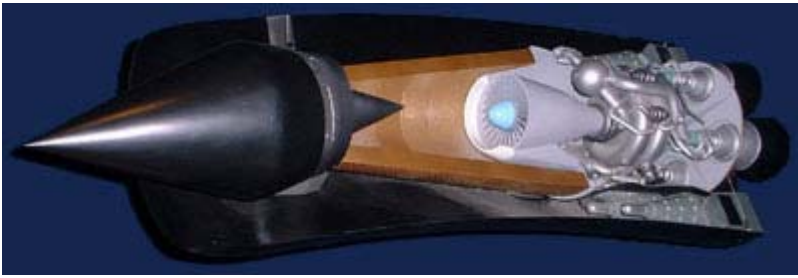
For some terrific illustrations and a lot more information on these engines, see the NASA web site:

<http://www.grc.nasa.gov/WWW/K-12/airplane/shortp.html>

...Now, don't you think the other engine pages are a lot more fun?

A Hybrid Airbreathing / Rocket Engine, Sabre Represents a Huge Advance over LACE Technology.

In the past, attempts to design single stage to orbit rockets have been unsuccessful largely due to the weight of oxidiser such as liquid oxygen. To reduce the quantity of oxidiser that a vehicle is required to carry it is (one possible solution) useful to be able to use atmospheric oxygen in the combustion process. The Sabre engine does this, allowing two mode operation - both airbreathing and conventional rocket type operation. This is made possible through a synthesis of elements from rocket and gas turbine technology.

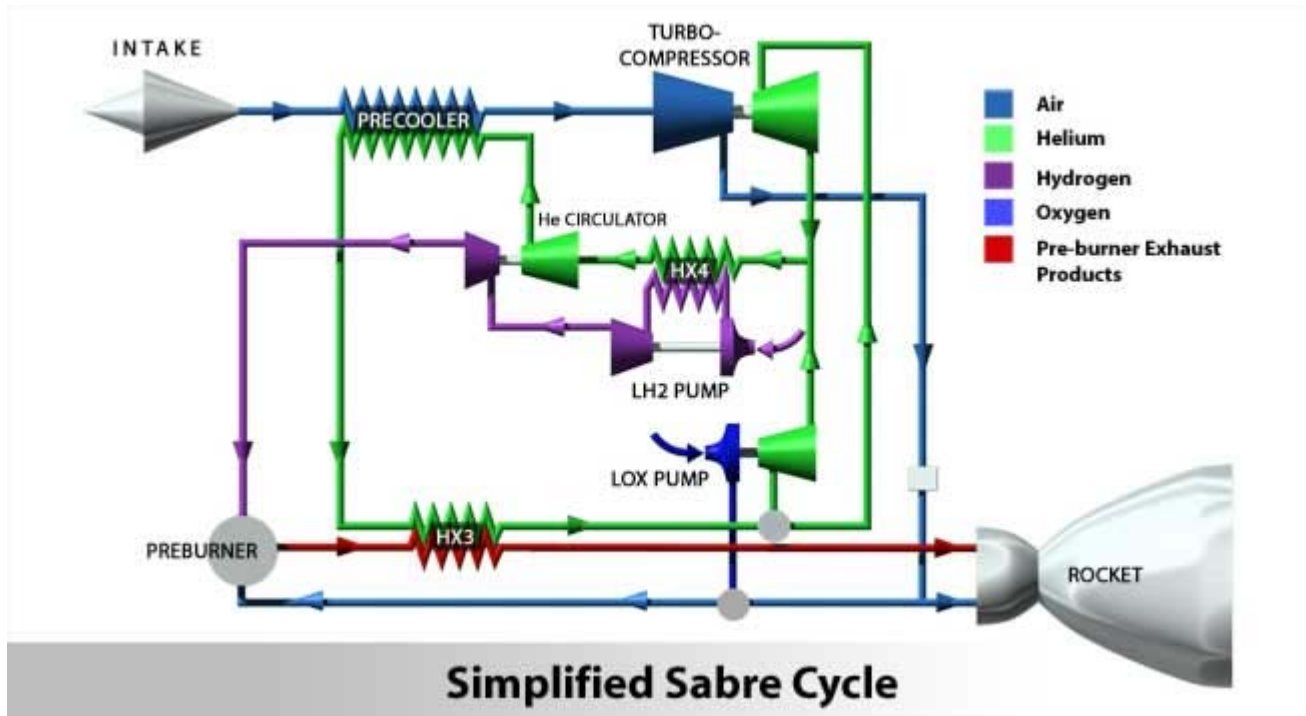


Model of the Sabre engine

The design of Sabre evolved from liquid-air cycle engines (LACE) which have a single rocket combustion chamber with associated pumps, preburner and nozzle which are utilised in both modes. LACE engines employ the cooling capacity of the cryogenic liquid hydrogen fuel to liquefy incoming air prior to pumping. Unfortunately, this type of cycle necessitates very high fuel flow.

These faults are avoided in the Sabre engine, which only cools down the air to the vapour boundary and avoids liquefaction. This allows the use of a relatively conventional turbocompressor and avoids the requirement for an air condenser.

The Sabre engine is essentially a closed cycle rocket engine with an additional precooled turbo-compressor to provide a high pressure air supply to the combustion chamber. This allows operation from zero forward speed on the runway and up to Mach 5.5 in air breathing mode during ascent. As the air density falls with altitude the engine eventually switches to a pure rocket propelling Skylon to orbital velocity (around Mach 25).



Air collection is via a simple conical two shock inlet with a translating centrebody to maintain shock-on-lip conditions. The centrebody moves forward to close the inlet for re-entry. A bypass system is used to match the variable captured air flow to the engine demand. This bypass flow is reheated in order to recover the momentum lost through the capture shock system.

The thrust during airbreathing ascent is variable but around 200 tonnes. During rocket ascent this rises to 300 tonnes but is then throttled down towards the end of the ascent to limit the longitudinal acceleration to 3.0g.

Rocket Exhaust Plume Phenomenology

Frederick S. Simmons

Chapter 1: Rocket Engines

1.1 Introduction

Understanding plume phenomenology requires some knowledge of rocket engines, their fundamental principles of operation, and their basic configuration. This chapter by no means constitutes a comprehensive treatment of the subject nor even an in-depth introduction. For that, the reader should refer to the classic text by George Sutton^{1,1} or a comparable source. Here the subject is reviewed to the extent necessary to provide missile defense system engineers and phenomenologists the fundamental parameters characterizing engine performance, particularly their effect on the observable attributes of the plume.

This chapter is divided into two parts. First, basic concepts and ideal engines are considered. Ideal in this context refers to the processes of operation characterized by one-dimensional isentropic fluid-mechanical relations. The content is restricted to those aspects of the flow that have a direct effect on the characterization of exhaust properties. The second part is devoted to the attributes of real engines that affect the reliability of plume properties based on the assumption of ideal combustion and flow processes.

1.2 Ideal Engines

1.2.1 Principles of Operation

A chemical rocket engine is a device for generating thrust by high-pressure combustion of propellants, that is, reactants, carried aboard the vehicle. The propellants are contained either in separate tanks as liquid fuels and oxidizers or in the combustion chamber itself, combined as a solid-propellant grain.* Thrust is consequent to the expansion of the combustion products through an exhaust nozzle. The *gross thrust* derives from the imbalance of pressure forces within the engine as shown schematically in Fig. 1.1. Within the combustion chamber, high pressure is produced by the reaction of the propellants. The pressure forces on the walls are balanced radially but not axially; the principal component of the thrust results from the force acting on the forward end of the chamber not balanced by an opposing force at the other end. That force acts on the gaseous combustion products that are accelerated to supersonic velocities through a converging-diverging (*De Laval*) nozzle.

A second increment of thrust is generated by the imbalance of the longitudinal components of the pressure forces normal to the diverging section of the nozzle. The gross thrust is invariant with altitude provided the flow in the nozzle does not separate from the walls. The *net thrust* is slightly less; the difference is the integral of the atmospheric pressure over the external surface of the engine. Consequently, the net thrust increases with altitude to an asymptotic limit termed the *vacuum thrust*. (Aerodynamic drag on the engine is treated separately as part of the drag on the vehicle that also depends on the ambient atmospheric pressure.) The mathematical basis for quantifying the various components of thrust is presented in a number of texts;^{1,1} the basic relations are discussed in Subsec. 1.2.3.

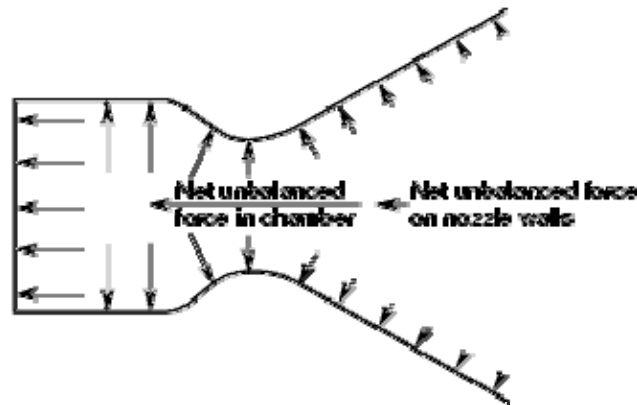


Fig. 1.1. Imbalance of forces in a rocket engine.

1.2.2 Engine Types

All rocket engines generate their thrust consequent to high pressures generated by propellant combustion. The simplest engines, usually designated as motors, utilize solid fuels and oxidizers blended into a more or less homogeneous mixture, cast into the pressure-containing structure of the motor casing, as illustrated in Fig. 1.2. As the propellants are consumed, the chamber pressure and hence the thrust vary somewhat with time. Solid-propellant motors normally are not throttleable or restartable; the combustion once initiated continues until the propellant is depleted.

A comparably simple engine uses pressure-fed liquid propellants, as indicated in Fig. 1.3. In this case, the tanks must be pressurized to a level higher than that in the combustion chamber; flow and combustion are initiated by the opening of valves in the propellant lines. (For hypergolic propellants, ignition is spontaneous; otherwise, an igniter of some sort is required. Frequently, initial injection of a small amount of a hypergolic combination is used as a starter.) Obviously, the walls of the tanks of a pressure-fed engine must be strong hence relatively heavy. Consequently, such liquid-propellant engines have found application only at very low thrust levels, for example, as required for space maneuvering where the weight of the tanks can be tolerated in the interest of simplicity and reliability. A *hybrid* engine, Fig. 1.4, uses a solid grain with a liquid oxidizer (or vice versa). This concept to some degree combines the simplicity of a solid propellant motor with the controlled combustion of a liquid propellant. There have been a number of such engines constructed and tested, but not used to date in any space or missile application.

Large liquid propellant engines used in the older long-range missiles or space launch vehicles are configured as illustrated in Fig. 1.5. The propellants are carried in tanks at pressures only sufficient to control the flow into gas-turbine driven pumps that increase the pressure to the necessary levels

for introduction into the chamber. *Gas generators* that provide the working fluid utilize the same propellants as the engine itself, but at a much fuel-richer mixture, hence a lower combustion temperature that can be tolerated by the turbine blades. In an *open-cycle* engine, these fuel-rich combustion products are exhausted in parallel with the main exhaust, obviously with an appreciable amount of unused energy. Modern liquid propellant engines are of the *closed-cycle* type illustrated in Fig. 1.6; the fuel-rich exhaust of the gas generator or *preburner* is reintroduced into the main combustion chamber where additional oxidizer is available. Thus, such engines operate with a higher overall combustion efficiency.



Fig. 1.2. Solid propellant motor.

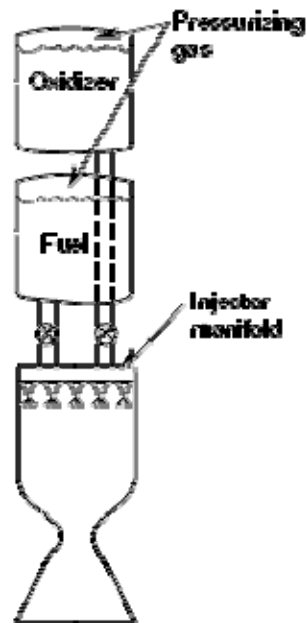


Fig. 1.3 Pressure-fed motor.

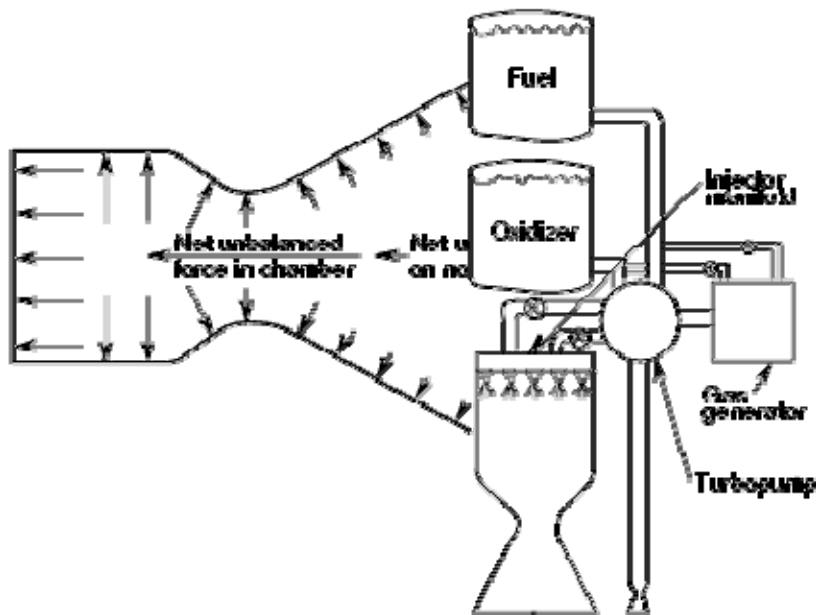


Fig. 1.4. Hybrid motor.

Fig. 1.5. Open-cycle engine.

1.2.3 Performance Parameters

Although the flow in a real rocket engine exhibits gradients in the radial and tangential directions, it is instructive to define various parameters by which performance is characterized in terms of a one-dimensional flow of combustion products.

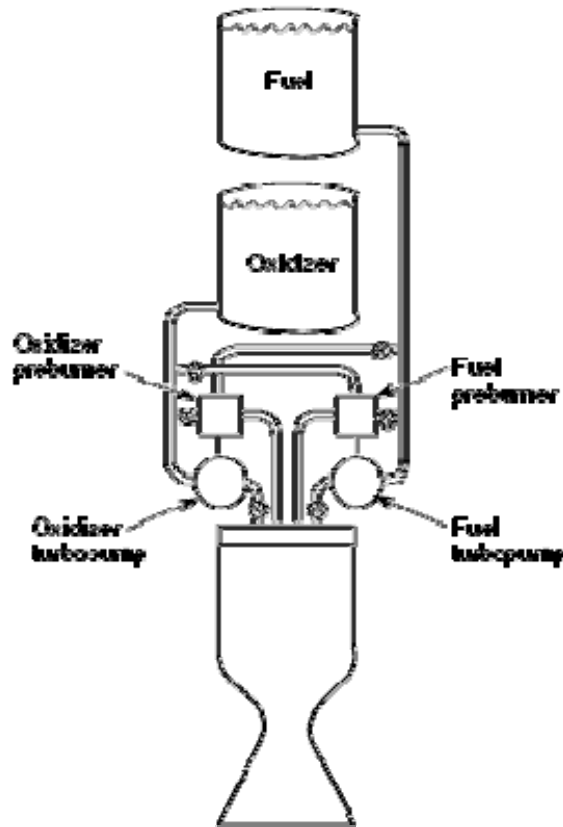


Fig. 1.6. Closed-cycle engine.

Accordingly, the basic expression for the thrust is derived from a simple balance of force and momentum:

$$F = \dot{m}V_e + (P_e - P_a)A_e \quad (1.1)$$

where F is the thrust, \dot{m} the mass flow rate, V_e , P_e , A_e are the velocity, static pressure, and area at the nozzle exit, and P_a is the ambient pressure. Both the exhaust velocity and the exit pressure depend on the nozzle expansion ratio; optimum performance occurs when the ambient and exit pressures are the same. If the exit pressure is less than the ambient, there is a loss in thrust; if the exit pressure exceeds the ambient, the full potential in thrust is not realized. The *design altitude* for a rocket engine occurs where the ambient pressure equals the exit pressure. However, the optimum nozzle expansion ratio for an engine designed for an upper stage involves a trade-off in the overall performance, because increasing the nozzle length also increases the engine weight. Usually, compromise results in the optimum expansion occurring at a fairly low value in the range of altitude for each stage in the flight of a ballistic missile.

Because the second term in Eq. (1.1) is relatively small, the exit or exhaust velocity is also a fundamental indicator of engine performance for a given propellant consumption rate. Preferable for that purpose, however, is the *effective exhaust velocity*, V_{eff} , defined by

$$V_{eff} = \frac{V_c + (P_c - P_a)A_t}{\dot{m}} \quad (1.2)$$

The customary index of performance is the specific impulse, I_{sp} , defined by

$$I_{sp} = \frac{\int_0^t F dt}{g \int_0^t \dot{m} dt} \quad (1.3)$$

where the numerator is the total impulse during the burn time t , the denominator is the total weight of propellant consumed during that period, and g is the acceleration of gravity at sea level. I_{sp} is expressed either in seconds in English units (thrust in pounds and propellant consumption in pounds/second) or metric units (Newtons and kilograms/second).

For solid propellants, both thrust and propellant consumption rate vary over the period of the burn so that Eq. (1.3) must be used to express the specific impulse. However, for liquid propellants over most of the burn of a given stage, the thrust and flow rates are constant, so that Eq. (1.3) reduces to

$$I_{sp} = \frac{F}{g\dot{m}} \quad (1.4)$$

from which it follows that

$$I_{sp} = \frac{V_{eff}}{g} \quad (1.5)$$

In other words, the effective exhaust velocity and the specific impulse are equivalent measures of engine performance.

Because thrust varies with the ambient pressure, so also does the specific impulse, which is frequently expressed in terms of the two limits: $I_{sp}(sl)$ and $I_{sp}(vac)$, referring to sea level and vacuum respectively. The former of course would only be applied to first stages.

The thrust of a rocket engine can also be expressed directly in terms of the imbalance in pressure forces

$$F = P_c A_t C_f \quad (1.6)$$

where P_c is the pressure in the chamber and A_t is the nozzle throat area. The dimensionless *thrust coefficient*, C_f , is defined by Eq. (1.6); in essence, it characterizes the contribution of the diverging section of the nozzle to the total thrust. Values of C_f typically range from 1.6 to 2.0 for nozzles of practical length.

Another quantity useful in characterizing rocket performance is the *characteristic exhaust velocity*, C^* , defined by

$$C^* = \frac{V_{eff}}{C_f} \quad (1.7)$$

and from Eqs. (1.4) and (1.6)

$$c^* = \frac{P_c A_c}{\dot{m}} \quad (1.8)$$

Equations (1.1) through (1.8) are the defining expressions for the performance parameters based on one-dimensional representations. All can otherwise be written in terms of fluid properties based on the assumption of isentropic flow through the nozzle:

$$V_c = \sqrt{\frac{2\gamma}{\gamma-1} RT_c \left[1 - \left(\frac{P_c}{P_c^*} \right)^{\frac{\gamma-1}{\gamma}} \right]} \quad (1.9)$$

where γ is the ratio of specific heats, R is the gas constant, T_c is the stagnation temperature at the nozzle inlet (i.e., the chamber temperature for a reasonable contraction ratio), and the velocity in the chamber is negligible compared to that at the exit. Isentropic flow relations can also be used to express the thrust, thrust coefficient, specific impulse, and characteristic velocity all in terms of the pressure ratio, specific heat ratio, and the combustion temperature.^{1,1} It is particularly instructive to do so for the characteristic velocity:

$$c^* = \frac{\sqrt{\gamma RT_c}}{\gamma \left(\frac{\gamma+1}{2} \right)^{\frac{\gamma-1}{2(\gamma+1)}}} \quad (1.10)$$

or

$$c^* = \sqrt{\frac{R_u}{M_m} f(\gamma, R_u, M_m)} \quad (1.11)$$

where R_u is the universal gas constant and M_m is the mean molecular weight of the combustion products. From the above relations, it follows that

$$I_{sp} \propto \sqrt{R_u / M_m} \quad (1.12)$$

which says that the maximum I_{sp} is realized at a mixture ratio such that the ratio of combustion temperature to molecular weight is a maximum. This mixture ratio is generally considerably lower than stoichiometric. The above result expressed in Eq. (1.12) also follows directly from the fact that, in expanding high temperature combustion products to a high velocity, thermal energy is converted into kinetic energy, that is,

$$nkT \rightarrow \frac{1}{2} m v^2 \quad (1.13)$$

Figure 1.7 shows a typical variation of I_{sp} with oxidizer/fuel (O/F) ratio for the common propellant combination of monomethyl hydrazine and nitrogen tetroxide. The optimum value for O/F, yielding the maximum I_{sp} , produces significant amounts of light molecules, for example, H_2 , CO , in the exhaust (see Chapter 4). It is not appropriate to characterize these products as "unburned fuel," which implies an inefficiency in combustion; they are products of the reaction of the fuel with the oxidizer even for a perfect combustion at the optimum mixture ratio. These combustion products are the primary source for the *afterburning* of plumes in the ambient atmosphere, a subject discussed in Chapter 3.

Note also in Fig. 1.7 that near the maximum, the specific impulse is a slowly varying function of mixture ratio and in particular does not degrade much with moderate departures from the optimum O/F. Accordingly, rocket engines are frequently designed to operate slightly fuel-richer than optimum to reduce the heat transfer to the nozzle. Another consequence of this attribute is that although inefficiency in combustion results in lower temperatures, so also mean molecular weights are lower so that changes in the ratio are not large and there is only a small penalty in specific impulse.

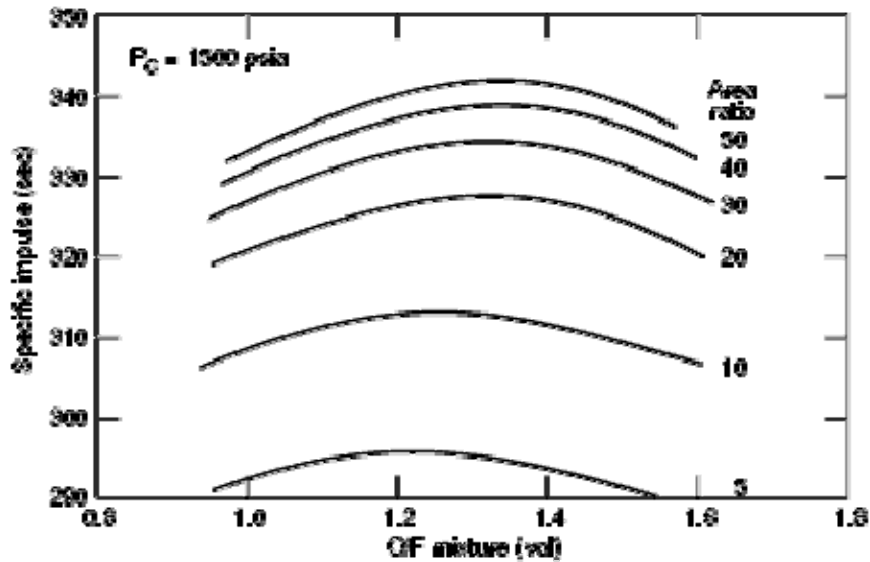


Fig. 1.7. Variation of specific impulse with mixture ratio.

1.2.4 Thrust Control

The thrust of a rocket engine of given dimensions is roughly proportional to the mass flow rate of the combustion products through the nozzle. In a liquid propellant engine, that rate is controlled simply by restricting the flow in the oxidizer and fuel lines leading to the injector assembly. Thrust termination or engine cutoff is accomplished by closing the valves in those lines. Control of thrust in a solid-propellant motor is quite different; the burning rate of the propellant varies directly and rapidly with the pressure at the surface where reaction is occurring. This behavior is expressed by the relation

$$\dot{\beta} = \alpha (T) P_c^n \quad (1.14)$$

where β is the burning rate, for example, inches/second, and P_c is the pressure at the surface of the grain. The coefficient α is a function of the initial temperature of the grain and the exponent n varies with the propellant formulation, typically with values between 0.2 and 0.8. Figure 1.8 illustrates this relation for a representative ammonium perchlorate solid propellant.^{1,2}

This relation at first would appear to represent an unstable condition regardless of the value of the exponent; as the pressure caused by the combustion builds up, the burning rate would continue to increase with time, thus precluding control. However, that is not the case. This can be illustrated by a simple argument (see Fig. 1.9).^{1,3} Assume a solid propellant motor is designed for a specified thrust at a nominal chamber pressure. The required nozzle area is then specified by means of Eq.

(1.6), from which the nozzle flow rate follows as a function of chamber pressure. The design then must specify the area of propellant burning surface for the required gas production rate to maintain the chamber pressure and thrust. Nonlinear gas production rates for hypothetical propellants exhibiting burning rates characterized by $n > 1$ and $n < 1$ at the nominal combustion chamber pressure are shown in Fig 1.9, together with the linear variation of the nozzle flow rate with the chamber pressure.

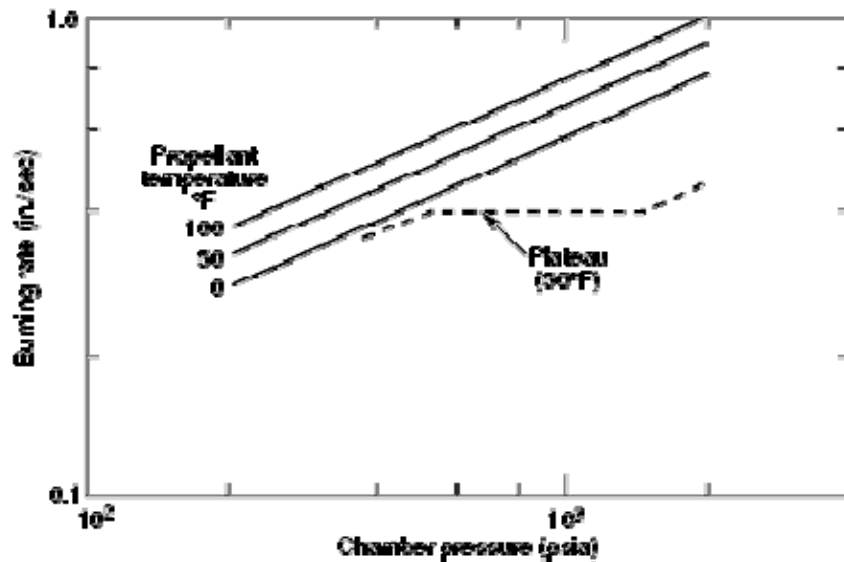


Fig. 1.8. Variation in burning rate of a solid propellant.

Consider the result of a small momentary decrease in chamber pressure. For $n < 1$, the gas generation rate exceeds the nozzle flow rate so that the pressure will tend to be restored; on the other hand, for $n > 1$, the pressure will continue to decrease. Conversely, for a momentary increase in chamber pressure, for $n < 1$ the gas generation rate is less than the nozzle flow rate, again producing a restoring effect. However, in this case $n > 1$ yields a higher gas production rate, thus further amplifying the effect. Hence, propellants characterized by $n < 1$ can be configured for stable combustion but not so for $n > 1$. (It would also follow that, for a propellant exhibiting a burn rate profile such as that indicated in Fig. 1.8 by $n > 1$, the pressure in the chamber would not build up at all after ignition.)

In real motors, two other effects are occurring simultaneously. The burning area will vary somewhat as the propellant is consumed, and the nozzle throat area can increase, for example, as the insulating liner ablates. The design of a solid propellant motor must account for all those effects to maintain a more or less constant chamber pressure.

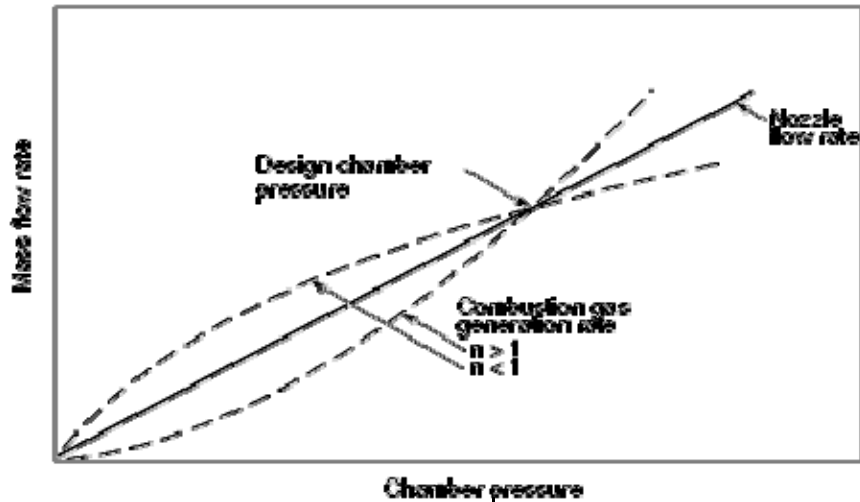


Fig. 1.9. Criterion for stability in solid propellant combustion.

Some earlier research studies were devoted to the development of *plateau* propellants, that is, with a plateau in the burning rate relation, as indicated by the dashed line in Fig. 1.8; this can be accomplished by adding certain compounds in the propellant mix.^{1.3,1.4} However, such propellants have not been widely pursued. Current practice relies on the behavior of conventional propellants with a burning rate characterized by an exponent considerably less than unity. For example, for the propellant in the solid rocket motor units of the space shuttle, the exponent is about 0.31.

The design for a reasonably constant thrust level during the burn then requires consideration of the rates of change in throat area and burning surface area of the propellant grain. In regard to the latter, modern solid motors frequently are designed with rather complex cross sections for the propellant grains. A further complicating factor is the variation of the burning rate with the initial temperature of the propellant (Fig. 1.8), which is not necessarily subject to strict control.

Solid motor thrust cannot be controlled during the burn in the sense that a liquid engine can be throttled by action of valves in the propellant feed lines. Accordingly, solid motors are designed to burn essentially to propellant depletion. However, it is desirable to terminate the thrusting in a more controlled manner than that resultant to totally depleting the propellant grain. This is usually done by suddenly opening a number of ports in the chamber so that the burning rate drops rapidly.

A manifestation of this overall behavior of solid propellant combustion is a chamber pressure that never reaches an absolutely constant value as in a liquid-propellant engine. Moreover, the resultant chamber pressure is dependent to some degree on the initial temperature of the grain; burn time also would depend on that temperature. Nevertheless, the pressure in a properly designed solid motor would attain a level sufficiently constant and close enough to the nominal design value to provide a stable period of combustion and hence total impulse. A typical chamber pressure history would appear as in Fig. 1.10, which shows another characteristic feature, a much slower tailoff in thrust compared to a liquid propellant cutoff.

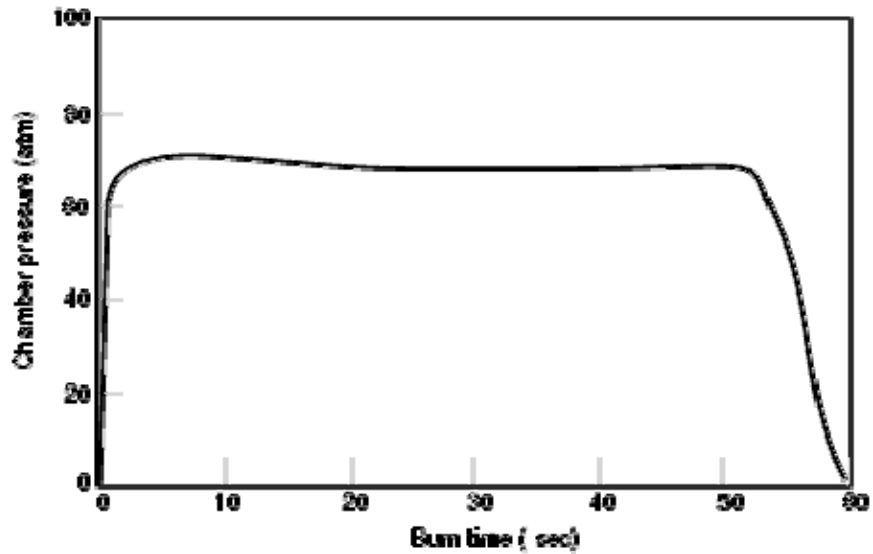


Fig. 1.10. Variation of chamber pressure in a solid propellant motor.

1.2.5 Thrust Vector Control

In addition to the thrust level, the thrust vector also must be controlled. There are four basic methods for achieving that control, as illustrated in Fig. 1.11. The whole engine or the nozzle assembly can be rotated by using a gimbal or swiveling mechanism. Heat-resistant vanes or other aerodynamic surfaces can be moved into the exhaust stream to deflect it. Alternatively, such deflection can be effected by injecting fluid through the wall of the diverging section of the nozzle. Otherwise, the thrust vector can be changed by rotating the entire missile by using auxiliary, for example, vernier, engines.^{*} The pros and cons of these various approaches are discussed in Sutton.^{1.1} Most modern launch vehicles employ gimballed nozzles for controlling the thrust vector. However, a number of current short-range missiles, descendants of the German V-2 rocket of World War II, use graphite vanes in the exhaust.

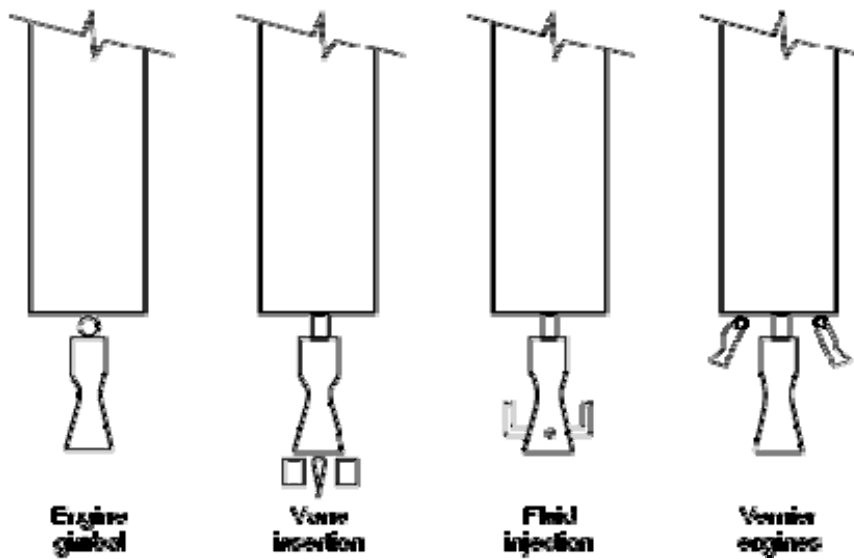
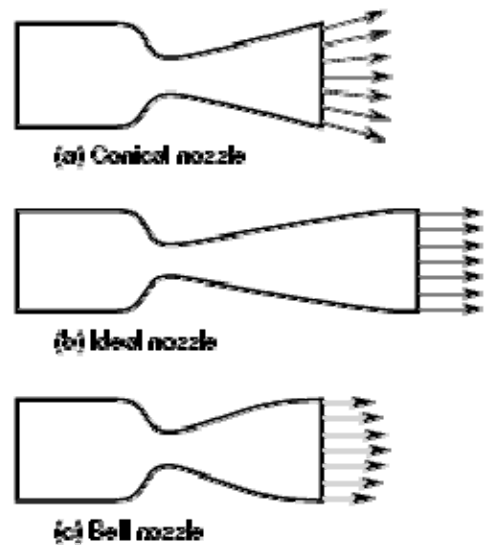


Fig. 1.11. Methods of thrust vector control.

The effect of these various methods for controlling the thrust vector on the observables of the plume of course depends on the magnitude of the change in exhaust flow direction induced. For very slight changes required to maintain a programmed flight path, the net effect on plume emission is correspondingly small. On the other hand a large change in exhaust flow direction relative to the flight path, that is, the missile velocity vector, could significantly increase the angle of attack and hence the infrared (IR) emission from the plume.

1.3 Real Engines

1.3.1 Three-Dimensional Flow



The assumption of a one-dimensional flow is useful for providing a basic understanding of the functioning of a rocket engine and for defining standard performance parameters. However, the flow in a real rocket engine departs from that ideal concept in three ways. First, the flow through a nozzle cannot be represented as one-dimensional. Consider a simple nozzle with a conical divergent section, as illustrated in Fig. 1.12(a). The flow at the exit plane is divergent hence inherently nonuniform. This divergence represents a loss in thrust, the radial components not contributing to the total. A closer approximation to an ideal one-dimensional nozzle would be one contoured to produce a uniform parallel flow at the exit plane, as indicated in Fig. 1.12(b). The shape of such a nozzle can actually be determined using a standard procedure for characterizing a supersonic flow, for example, the *method of characteristics*. However, for a real engine, such a nozzle would be very long hence unacceptably heavy. In engineering practice, the trade-off in nozzle weight versus increased thrust for an overall optimization results in a bell-shaped nozzle, Figure 1.12(c), in which the exit flow is nearly parallel but necessarily nonuniform in velocity and other properties. Methodology for the optimization of the nozzle wall contour was developed by G.V.R. Rao at Rocketdyne;^{1,5} it involves the matching of the expansion waves generated just downstream of the throat with the compression waves created as the flow is turned further downstream, thus to minimize the losses.^{1,1}

Fig. 1.12. Nozzle shapes.

Up to this point, the term ideal flow has referred to one-dimensional isentropic representation, in which properties at any station along the flow in the chamber and nozzle are considered to be uniform and in both thermal and chemical equilibrium. It is convenient now to extend that definition of ideal to include representations in which various two-dimensional (axisymmetric) nonequilibrium effects can be treated by well-developed methodology, such as that described in Chapter 5. This permits definitions of efficiency in terms of the ratios of measured performance to theoretical performance. Thus, a combustion efficiency η_c can be defined as

$$\eta_c = \frac{C^*}{C^*_{theor}} \quad (1.15)$$

and a nozzle efficiency as

$$\eta_n = \frac{C_f}{C_{f,theor}} \quad (1.16)$$

where the theoretical values are those predicted by the Joint Army-Navy-NASA-Air Force one-dimensional equilibrium (JANNAF ODE) code (see Chapter 4).

1.3.2 Nozzle Expansion Ratio

The flow in the supersonic section of the nozzle will expand to a pressure dependent on the ratio of the exit plane area to the throat area. If the exit pressure is greater than the ambient pressure, the exhaust will immediately expand until the static pressure in the stream adjusts to its surroundings. In this case the thrust coefficient is somewhat less than that for a longer nozzle. Conversely, if the exit plane pressure is less than ambient, the exhaust stream will contract. In this case there is a decrement of thrust in accordance with Eq. (1.1). The condition of equal pressure is encountered at the design altitude. These three conditions are illustrated in Fig 1.13 along with a fourth, in which the exit pressure is so much lower than the ambient pressure that the flow within the nozzle separates from the wall.

The nozzle of a particular stage of a ballistic missile is configured to maximize total impulse as the vehicle rises and passes through the design altitude. Obviously, an upper-stage engine will incorporate a nozzle of greater expansion ratio, with the limiting factor being the burden of additional weight. Of course, a long-range missile will rise far above the design altitude of its uppermost stage. The behavior of the exhaust expanding into ever-diminishing pressure is discussed in Chapter 2.

If a rocket engine is statically tested on the ground, the nozzle exit pressure will invariably be less than the one atmosphere of the surroundings, and the plume will necessarily contract. If the design exit pressure is not too much less than an atmosphere, the nozzle will flow full and the gases will overexpand and then contract outside the nozzle. This characteristic permits diagnostic measurements of exit plane properties during such testing that are then applicable to the plume of the missile in flight. However, if the nozzle expansion ratio is too great, as for an upper-stage engine in a sea-level test, the flow will separate from the nozzle wall, and a recirculation region will form inside the nozzle along with a system of oblique shock waves. This condition is also illustrated in Fig 1.13. In this case the nozzle exit properties would differ considerably from those at or above the design altitude.

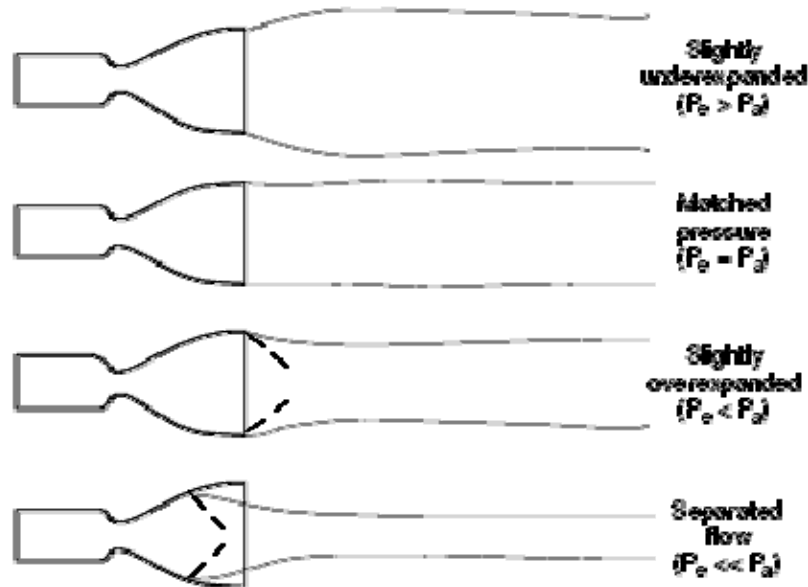


Fig. 1.13. Nozzle flow in static testing.

1.3.3 Unmixedness

The combustion and flow processes in real rocket engines are only approximated by the one-dimensional relations defined above. In addition to the three-dimensional aspects of the flow (the divergence losses), there are other sources of inefficiency. These include viscous boundary layer losses, kinetic losses in the chemical reactions themselves, particulate drag losses, and losses in energy release caused by nonideal vaporization and mixing on a small scale. However, the most significant departure from the idealized flow as described above is consequent to two effects: the unmixedness of the reactants in the combustion chamber and, in the case of liquid propellants, incomplete vaporization. The latter effect is discussed in Subsec. 1.3.4.

In a real liquid-propellant engine, the fuel and oxidizer are introduced separately into the chamber through a large array of small impinging jets to form fine mists that quickly mix and react. (Commonly, the injector is designed to produce a uniform mixture ratio in the central region of the combustion chamber but a richer mixture near the wall to facilitate cooling.) In addition, throughout the chamber, there are local regions of nonoptimum O/F that result in gradients in temperature and variations in the mole fractions of the products. This effect, which persists through the chamber and nozzle, can produce striations in the exhaust that in some cases can be related to the pattern of holes in the injector. Figure 1.14 is a photograph of the exhaust of an Atlas booster engine showing such streakiness. Figure 1.15 is a better example of that effect, an image produced by an infrared camera (3–5 μm) of a Delta liquid-propellant core stage at about 96 km altitude, viewed from the ground. The radial streaks, attributable to the injector pattern, are more or less stationary; the tangential pattern is nonstationary and consequent to fluctuations in the flow. These effects can yield conditions in the exhaust leading to significant departures of the predicted radiative properties of plumes based on assumptions of well-mixed gas-phase reactions.

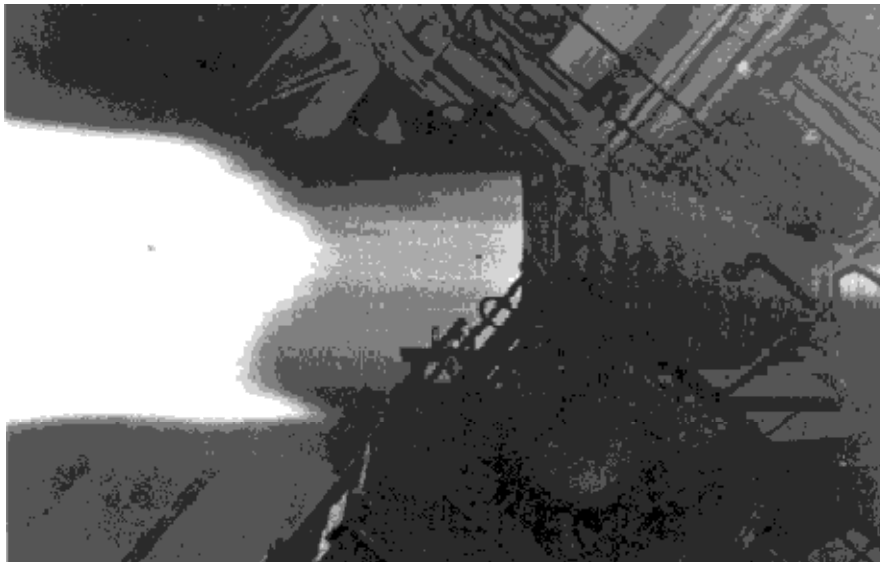


Fig. 1.14. Striations in the exhaust from an Atlas booster engine.
(Courtesy Boeing Rocketdyne.)

In a solid-propellant engine, the effects of unmixedness are coupled to a characteristic temporal unsteadiness. For one thing, there are small-scale inhomogeneities in the propellant mix, and the burning rate is not perfectly constant, influenced by variations in the local pressure along the length of the chamber. Not only are there spatial inhomogeneities in the resultant combustion products, but also finite-sized chunks of unburned grain can be intermittently ripped off the surface and carried in the flow. Some of these chunks are large enough that on occasion their burning extends into the exhaust. In addition, liquid alumina, produced in the combustion, can accumulate in nooks and crannies in the motor and be blown out intermittently, likewise producing momentary flashes. The latter effect is considered by some analysts to be the dominant source of nonuniformity in a solid-propellant exhaust.

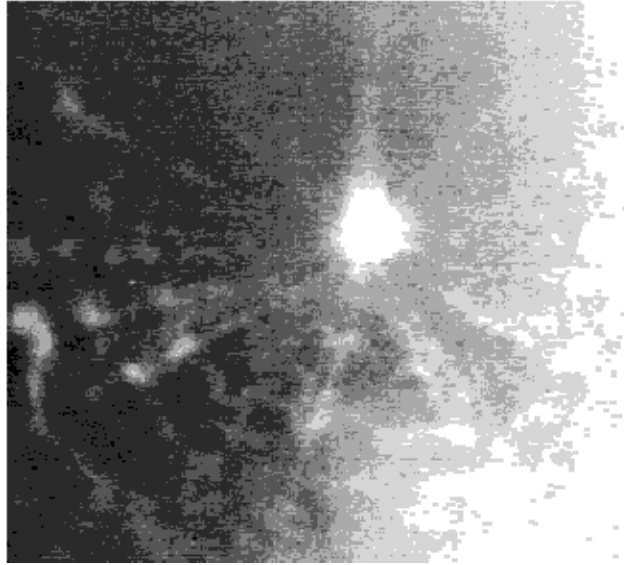


Fig. 1.15. Image of Delta core stage viewed from the rear. (Courtesy ISTEf.)

1.3.4 Incomplete Vaporization

A comparable source of inefficiency in the performance of a real engine is that of incomplete vaporization of one or both propellants. In general, vaporization of droplets, usually the fuel, is the rate-limiting factor in the combustion of liquid propellants; a theoretical representation of this effect was provided many years ago by Richard Priem and his associates at the NASA Lewis Laboratory.^{1,6} Figure 1.16 illustrates the process of a burning in a liquid-propellant rocket chamber. Droplets of fuel and oxidizer are produced by the impingement of liquid streams, usually like-on-like, from the injector. These droplets, surrounded by gaseous products of prior combustion, initially moving at higher velocity than the gas close to the injector face, at first are accelerated by drag to the gas velocity, and then lag the rapidly expanding gaseous products. In general the droplets are heated convectively, evaporate, and react with the vapor of the other propellant. For simplicity, Fig. 1.16 represents the place where the velocities are matched so that the flame front is approximately spherical. Thus, heat is transported inward while fuel vapor moves radially outward from the droplet, there to encounter an oxidizer-rich local environment. The droplet essentially remains at the boiling point until it is finally consumed; the downstream point of disappearance will depend on droplet size. The rate of droplet vaporization has been established to be the rate-controlling process in liquid-propellant combustion.^{1,7}

There are, of course, steep radial gradients in temperature and composition from the droplet to the free stream. Consequently, hydrocarbon fuel vapor can be heated to the cracking point before the reaction, thus producing carbon as a product not predicted for the overall mixture ratio and persisting as soot particles through the subsequent mixing and acceleration. This process is discussed further in Chapter 9.

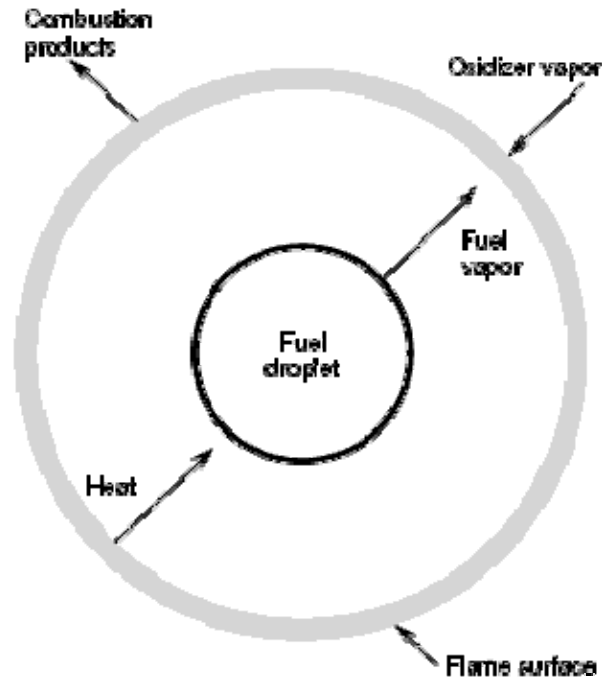


Fig. 1.16. Flame front of a burning droplet. 1.8

As a further departure from ideal well-mixed gaseous combustion, the spray from impinging streams of hypergolic propellants can be interrupted by the highly unsteady reactions occurring near the injector face, resulting in substantial numbers of relatively large droplets. The liquid vaporization rate diminishes with the reduction in convective heat transfer as the droplets are accelerated by the gaseous products in their motion toward the nozzle. Thus, a fraction of the mass flow entering the nozzle could be unevaporated and of course unreacted. However, the particles are unlikely to survive the highly turbulent shearing forces through the nozzle. (Although propellant droplets are sometimes seen in the exhaust of small, relatively inefficient thrusters used for attitude control or orbital maneuvering, they are not evident in the exhaust of large booster engines.) The net effect of this unevaporated liquid is an effective O/F ratio for the gaseous phase reaction closer to stoichiometric than the nominal O/F for the chamber. This can result in considerably higher temperatures at the nozzle exit than predicted by the standard performance codes for the nominal mixture ratio; this is discussed in Chapters 5 and 10.

1.3.5 Cooling

Another source of departure from the ideal is the cooling of the chamber walls, which introduces strong gradients in gas temperature through the boundary layer. Cooling of course is necessary; the combustion temperatures greater than 3000 K and chamber pressures of more than 130 atmospheres introduce an enormous heat transfer load. Three methods, frequently in combination, are used for the chambers and nozzles of liquid-propellant engines: *regenerative, film, and radiative cooling*, as illustrated schematically in Fig. 1.17. Combustion efficiency loss in regenerative cooling is minimized because some of the energy loss is recaptured in the coolant propellant (which is then introduced into the chamber at a higher temperature). In film cooling some engines, fuel is sprayed on the chamber wall through an annular array of nonimpinging streams from the injector. In others, the outermost sets of impinging jets are configured to produce a relatively rich mixture. In either case, a much lower combustion temperature results in the peripheral zone of the chamber, thus

reducing the heat transfer. In radiative cooling, the chamber walls are constructed of materials capable of maintaining their structural integrity and strength at very high temperatures. This method is usually restricted to engines of very low thrust. In solid-propellant motors, the chamber walls are protected by a layer of insulation. Furthermore, they are thick enough to keep their strength at considerably elevated temperatures.

Rocket engine nozzles also require cooling. Although the gas temperature and pressure drop rapidly through the nozzle, the heat transfer varies directly with the product of the density and flow velocity. Moreover, as a consequence of viscous effects in real gases, the *recovery* temperature in the boundary layer is closer to the *stagnation* temperature than to the *static* temperature of the free stream. The net effect is that the maximum heat transfer rate occurs at the nozzle throat. Nozzles are cooled by one or more of the methods outlined above, frequently in combination with a fourth method, *ablative* cooling. In this method, the nozzle wall is lined with a high-temperature insulating material that gradually erodes, thus carrying off much of the heat transferred to the wall. In some liquid-propellant engine nozzles, a regeneratively cooled section is joined to a downstream section that is ablatively or radiatively cooled. Nozzles of solid-propellant motors are usually constructed with a high-temperature material such as graphite forming the throat, frequently in combination with ablative materials lining the converging and diverging sections.

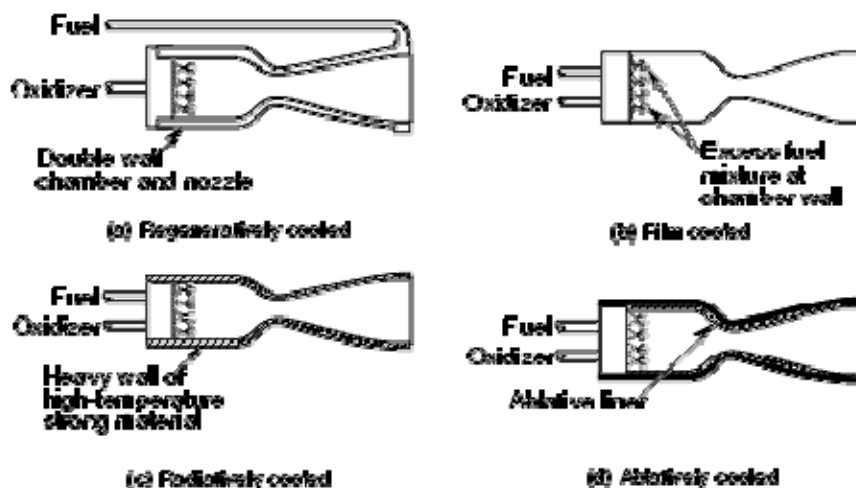


Fig. 1.17. Methods of nozzle cooling.

1.3.6 Exit Plane Properties

An important consequence of these attributes of real engines lies in the departure of nozzle exit flow properties from the ideal or theoretically calculated values. Inefficiencies in the combustion process tend to produce significantly different temperatures and molecular weights in the products; this results in a small and tolerable reduction in specific impulse (Fig. 1.17). However, there can be substantial impact on the properties of plumes calculated using theoretically derived nozzle exit properties as input.

Where possible, actual nozzle exit properties should be determined experimentally. The usual method involves multispectral measurements of the IR emission and absorption in their variation with offset from the plume axis. By one of several inversion techniques, the radial profiles in temperature and partial pressures of the emitting species can be extracted. This subject is elaborated

in Chapter 10. Alternatively, real engine effects ought to be included in theoretical methods for defining exit conditions as input to plume models, as indicated in Chapter 5.

1.4 References

- ^{1.1}G. P. Sutton, *Rocket Propulsion Elements*, 6th ed. (John Wiley and Sons, Inc., New York, 1992).
- ^{1.2}M. Shorr and A.J. Zaehring, *Solid Rocket Technology* (John Wiley and Sons, New York, 1967).
- ^{1.3}N. Kubota, "Survey of Rocket Propellants and Their Combustion Characteristics," in *Fundamentals of Solid-Propellant Combustion*, K. Kuo and M. Summerfeld, eds., Vol. 90 of *Progress in Astronautics and Aeronautics* (AIAA, New York, 1984).
- ^{1.4}E. K. Bastress, "Modification of the Burning Rates of Ammonium Perchlorate Solid Propellants by Particle Size Control," Ph.D. thesis, Princeton University, 1961.
- ^{1.5}G.V.R. Rao, "Exhaust Nozzle Contour for Optimum Thrust," *Jet Propulsion* 28, 377 (1958).
- ^{1.6}R. J. Priem and M. F. Heidmann, "Propellant Vaporization as a Design Criterion for Rocket Engine Combustion Chambers," NASA Technical Report R-67, 1960.
- ^{1.7}W. T. Olsen, "Problems of High-Energy Propellants for Rockets," *Rocket and Missile Technology*, Chemical Engineering Progress Symposium Series, Vol. 57, No. 33, American Institute of Chemical Engineers, 1961.
- ^{1.8}R. S. Levine, "Some Considerations of Liquid Propellant Combustion and Stability," *Rocket and Missile Technology*, Chemical Engineering Progress Symposium Series, Vol. 57, No. 33, American Institute of Chemical Engineers, 1961.

Rocket Thermal Evaluation

RTE is a comprehensive Rocket Thermal Evaluation computer code developed for NASA Lewis Research Center, presently Glenn Research Center. The early version of the code was distributed through NASA's COSMIC Library. The COSMIC version of RTE is marketed by AP Poiner Inc. (<http://www.appioneer.com/products/11283.html>). The latest version of RTE can be purchased from Tara Technologies LLC (www.tara-technologies.com). The program has been modified substantially since its early version release. This page provides a brief description of the code. [For a brief slide presentation of this code with some sample results click on this text.](#) For manual of the latest version of RTE (RTE2002) [click on this text.](#)

SUMMARY

RTE (Rocket Thermal Evaluation) is a computer code for three-dimensional thermal analysis of regeneratively cooled rocket thrust chambers and nozzles. A unique feature of this code is conjugating all thermal/fluids processes in the propulsion system in order to obtain matched results for the thermal field. These thermal/fluids processes include: convection and radiation heat transfer from hot combustion gases to the liner of the engine; conduction heat transfer with walls; and convection to the coolant. RTE uses an iterative marching scheme to match the heat flux and temperature fields of these thermal processes. The program uses GASP (GAS Properties), WASP (Water and Steam Properties) and a module for properties of RP1 to evaluate coolant flow properties. Hence, it is capable of handling all commonly used coolants in propulsion systems (e.g., H₂, O₂, H₂O, CH₄ and RP1). CET (Chemical Equilibrium with Transport Properties) code is used for evaluation of hot gas properties. The inputs to RTE consist of the composition of fuel/oxidant mixtures and flow rates, chamber pressure, coolant entrance temperature and pressure, dimensions of

the engine, materials and number of nodes in different parts of the engine. It allows temperature variations in axial, radial and circumferential directions and by implementing an iterative scheme, it provides a listing of nodal temperatures, rates of heat transfer, and hot-gas and coolant thermal and transport properties. The O/F (oxidant/fuel) ratio can be varied along the thrust chamber. This feature allows the user to incorporate a non-equilibrium model or an energy release model for the hot-gas-side. The mixture ratio at each station can be calculated using ROCCID. Thermal radiation from hot gases within the chamber is also included in the analysis. The exchange factors for radiation calculations are evaluated using an external module (RTE_RAD, Rocket Thermal Evaluation Discrete Exchange Factor), which can be input to the main rocket thermal evaluation code.

This code can be used for both regeneratively and radiatively cooled engines. For regeneratively cooled engines, the code can be used for one pass as well as pass-and-half cooling cycles. Additionally, the blocked channel option allows a user to assess the thermal performance of a regeneratively cooled engine when a cooling channel is blocked. The user has the option of bypassing the hot-gas-side calculations and directly inputting gas side fluxes. This feature can be used to link RTE to a boundary layer program for the hot-gas-side heat flux calculation. The procedure for linking RTE to a hot-gas side program, TDK (Two Dimensional Kinetics Nozzle Performance Computer Program) is described in this manual.

RTE is written in Fortran and has been successfully compiled on a number of UNIX systems and Microsoft Windows. Shell programs have been developed for UNIX and WINDOWS operation systems to link RTE and TDK. To ease inputting the large data sets needed to run the program a Graphic User Interface (preprocessor) based on Excel is provided. A user can fill in engine specifications in designated Excel cells and choose the right engine information from combo boxes. Then by clicking on a command button, data from the Excel interface would be transferred into RTE's input file. [For a trial version of RTE's GUI click on this text if you are using internet explorer, or right click on this text and save the file if you are using Netscape. Then go to the Appendix D of RTE2002 manual for instructions on using RTE's GUI.](#) Also, RTE and its radiation module can be run from Excel. RTE provides a number of output files, each provide useful information regarding the engine's thermal performance. The Graphic postprocessor of RTE is based on Tecplot software. It produces a number of output files that can be processed by Tecplot for temperature isotherms and graphic results.

SUMMARY OF THE NUMERICAL MODEL AND SOME SAMPLE RESULTS

The Rocket Thermal evaluation code is based on the geometry of a typical regeneratively-cooled engine similar to that shown in Figure 1.

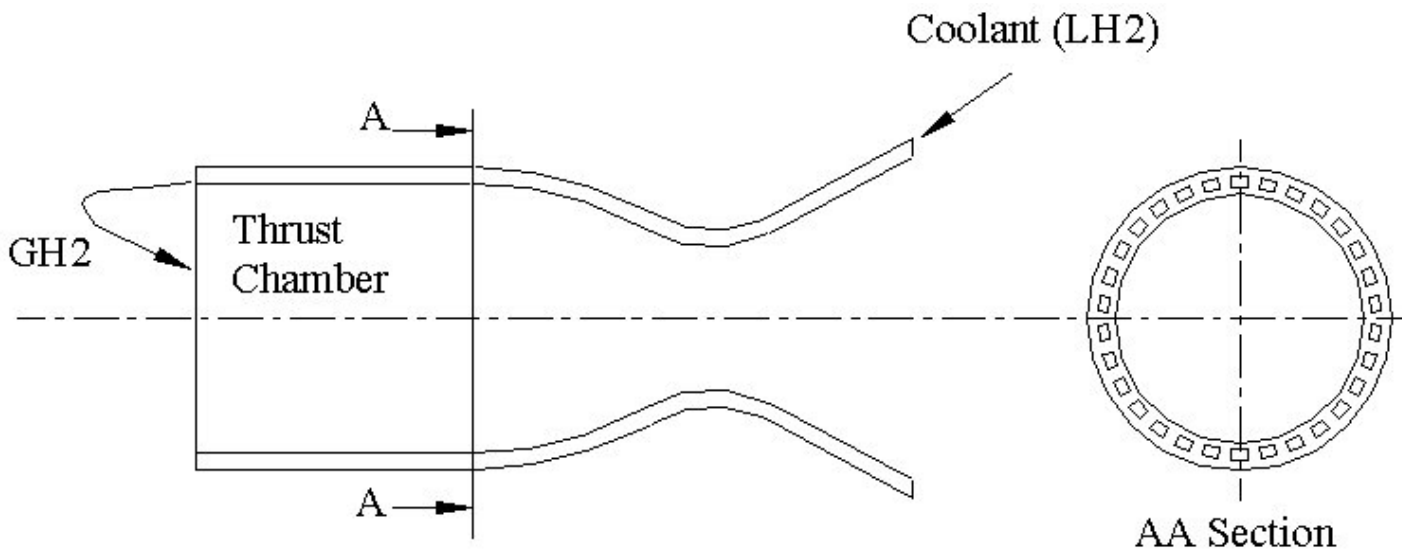


Figure 1: Configuration of a typical regeneratively cooled rocket thrust chamber and nozzle

The wall can consist of three layers: a coating, the channel, and the closeout. These three layers can be different materials or the same material. The number of cooling channels in the wall are also specified by the user. For the numerical procedure, the rocket thrust chamber and nozzle are subdivided into a number of stations along the longitudinal direction, as shown in Figure 2.

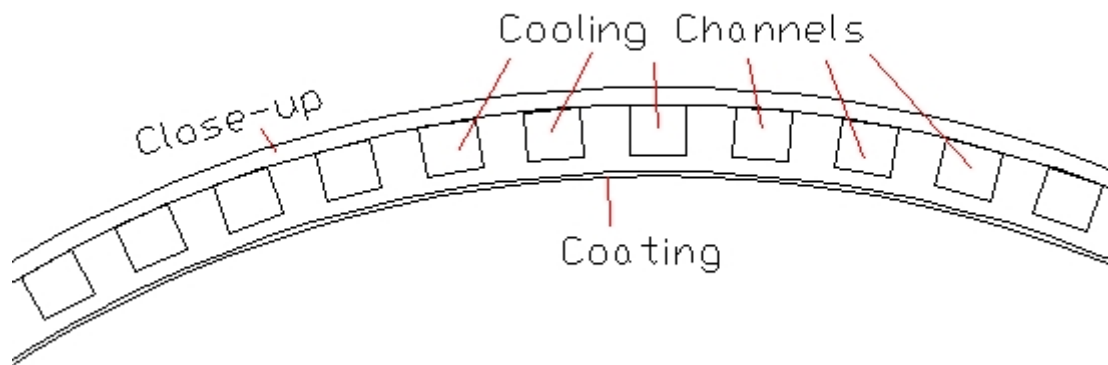


Figure 2: Configuration of a typical regeneratively cooled thrust chamber and nozzle wall

The wall can consist of three layers: a coating, the channel, and the closeout. These three layers can be different materials or the same material. For the numerical procedure, the rocket thrust chamber and nozzle are subdivided into a number of stations along the longitudinal direction, as shown in Figure 3. The thermodynamic and transport properties of the combustion gases are evaluated using the chemical equilibrium composition computer program developed by Gordon and McBride (CET, Chemical Equilibrium with Transport properties). The GASP (GAS Properties) or WASP (Water And Steam Properties) WASP} programs are implemented to obtain coolant

thermodynamic and transport properties. Since the heat transfer coefficients of the hot gas and coolant sides are related to surface temperatures, an iterative procedure is used to evaluate heat transfer coefficients and adiabatic wall temperatures.

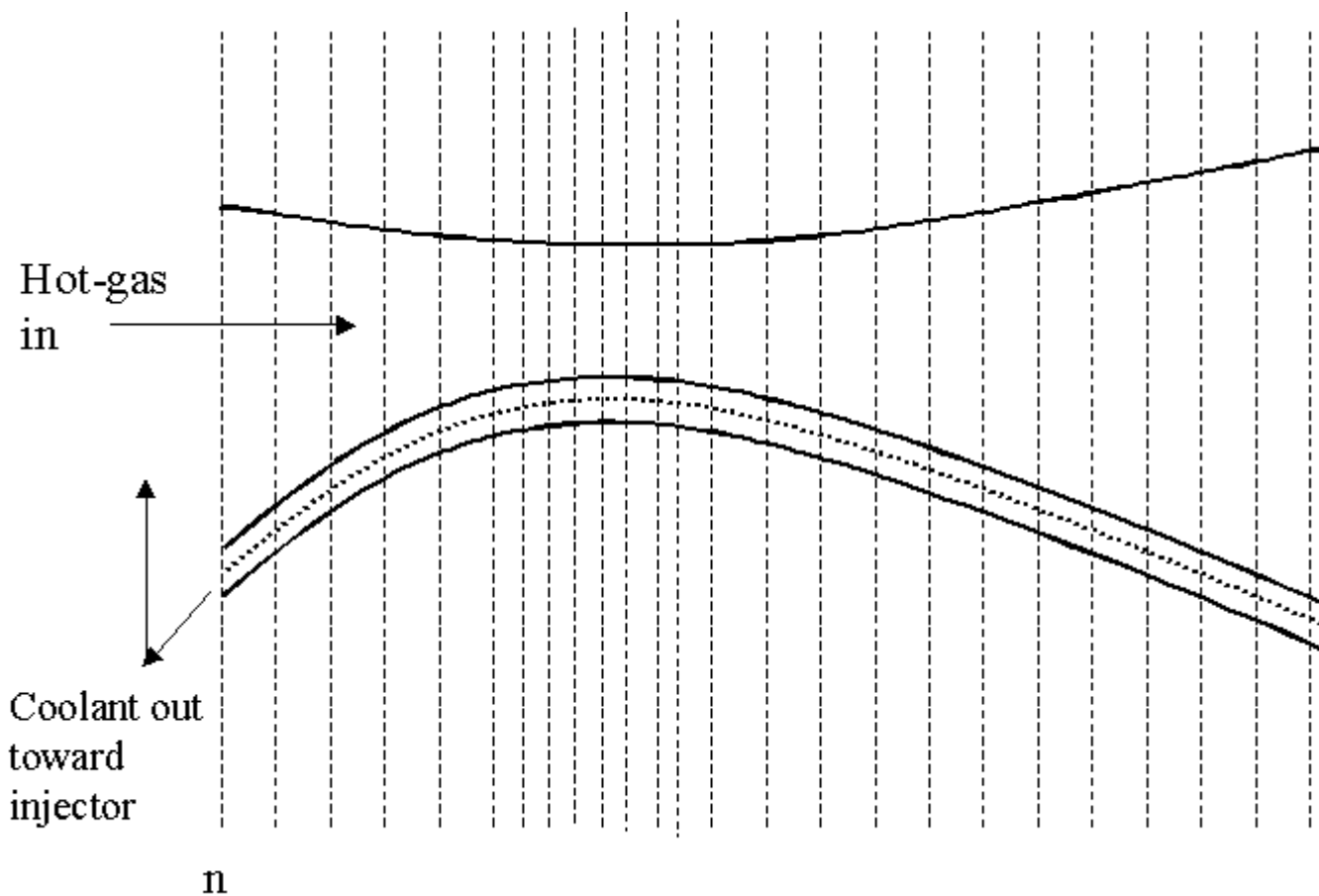
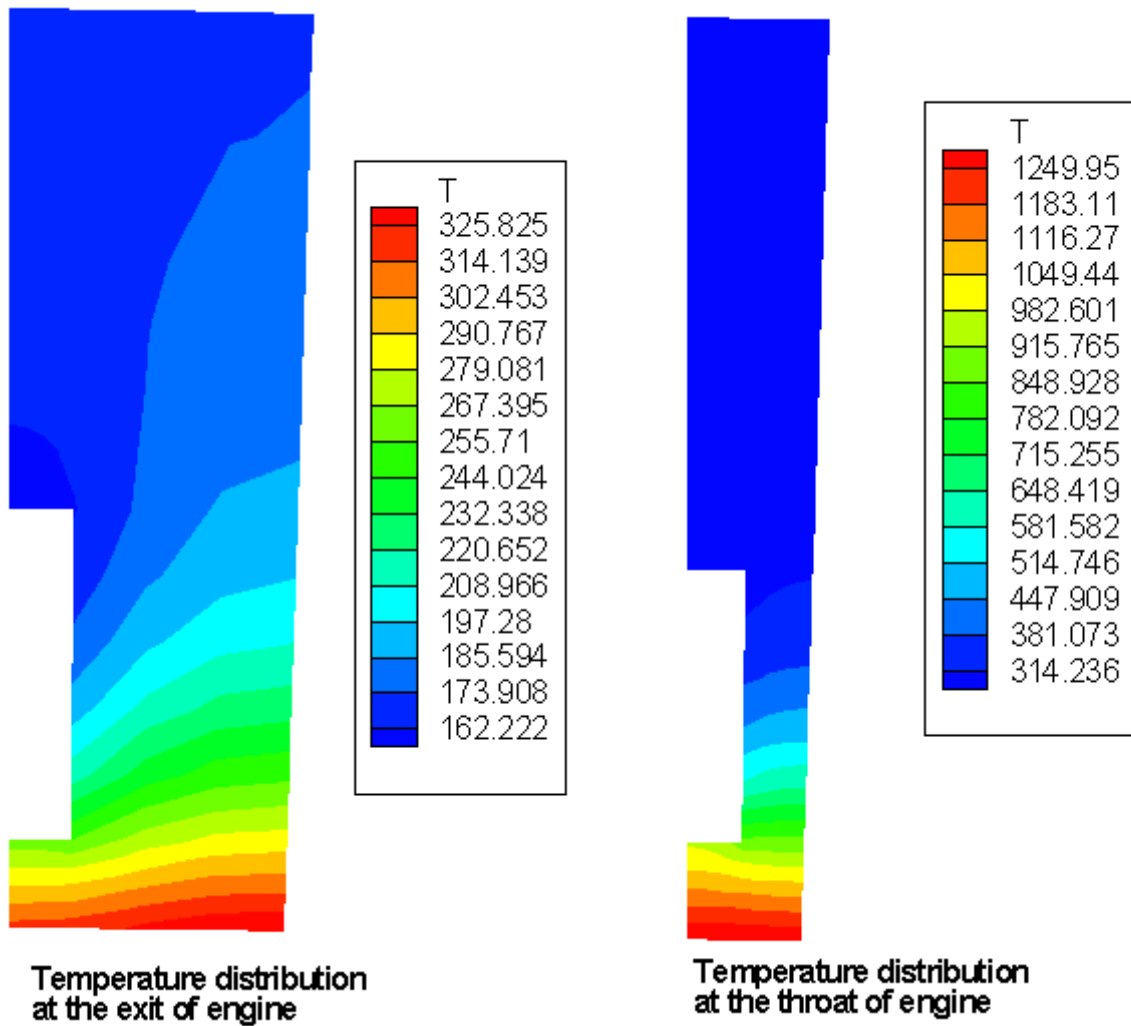


Figure 3: A rocket thrust chamber and nozzle subdivided into a number of stations

The temperature distribution within the wall is determined via an axial marching technique starting from station 1 to the last station. The program marches axially from one station to another. At each station a two-dimensional finite element model is used to determine the temperature distribution along the radial and circumferential directions. The axial heat conduction acts as internal heat source in the two-dimensional heat conduction model. When the axial march is completed, comparison is made between the results of the present march and that of the previous one to see if the convergence criteria in the axial direction has been met. If it is not met, the code starts again at the first station and makes another axial march. The process continues until convergence is achieved. A detailed description of this numerical model is outlined in the manual of RTE.

The following figures show some sample results of the rte (wall temperature distribution at various locations in the engine). Note that the temperature distribution is given for one cell and the indentation at the left is the cooling channel.



Similar temperature distributions can be generated for all stations along the engine. In addition to the wall temperature distribution the program provides all transport and thermodynamics properties for coolant and combustion gases.

More detailed information on this program can be obtained from the following publications:

- [Naraghi, M.H.N., "RTE - A Computer Code for Three-Dimensional Rocket Thermal Evaluation," User Manual, 2002.](#)
- Naraghi, M.H.N., "RTE - A Computer Code for Three-Dimensional Rocket Thermal Evaluation," Grant NAG 3-892 report, prepared for NASA Lewis Research Center, 1994.
- Naraghi, M.H.N., "RTE - A Computer Code for Rocket Thermal Evaluation," presented at the 1994 Thermal and Fluid Analysis Workshop, Cleveland, Ohio, August 15-19, 1994.
- Hammad, K.J., and Naraghi, M.H.N., "Radiative Heat Transfer in Rocket Thrust Chambers and Nozzles," **AIAA paper 89-1720**, presented at the 24th AIAA Thermophysics Conference in Buffalo, New York, June 12-14, 1989; also **AIAA Journal of Thermophysics and Heat Transfer**, Vol. 5, No. 3, pp. 327-334, 1991.

- Naraghi, M.H.N., and Armstrong, E.S., "Three Dimensional Thermal Analysis of Rocket Thrust Chambers," **AIAA paper 88-2648**, presented at the AIAA Thermophysics, Plasmadynamics and Lasers Conference, San Antonio, Texas, June 27-29, 1988.
- Naraghi, M.H.N., and DeLise, J., "Conjugate Conductive, Convective and Radiative Heat Transfer in Rocket Engines," **ASME publication HTD-Vol. 307**, pp. 65-79, Preceding of the 30th National Heat Transfer Conference, Portland, Oregon, August 6-8, 1995.
- [Delise, J.C., and Naraghi, M.H.N., "Comparative Studies of Convective Heat Transfer Models for Rocket Engines," AIAA paper 95-2499, presented at the 31st AIAA/ASME/SAE/ASEE Joint Propulsion Conference and Exhibit, San Diego, CA, July 10-12, 1995.](#)
- [Naraghi, M.H.N., Quentmeyer, R.J. and Mohr, D.H., "Effect of a Blocked Channel on the Wall Temperature of a Regeneratively Cooled Rocket Thrust Chamber," AIAA paper 2001-3406, presented at the 37th AIAA/ASME/SAE/ASEE Joint Propulsion Conference and Exhibit, Salt Lake City, UT, July 8-11, 2001](#)
- [Naraghi, M.H.N., and Nunes, E.M., "Effects of Gas Radiation on the Thermal Characteristics of Regeeratively Cooled Rocket Engines," ASME paper IMECE2002-33920, presented at the 2002 ASME International Mechanical Engineering Congress, New Orleans, Louisiana, Nov. 17-22, 2002](#)
- [Naraghi, M.H.N., Dunn, S. and Coats, D., "A Model for Design and Analysis of Regeneratively Cooled Rocket Engines," AIAA paper 2004-3852, presented at the Joint Propulsion Conference, Fort Lauderdale 2004](#)
- [Naraghi, et. al., Modeling of Radiation Heat Transfer in Liquid Rocket Engines, presentation at the Joint Propulsion Conference, Tucson, Arizona 2005](#)
- [Naraghi, M.H.N., Dunn, S. and Coats, D., "Dual Regenerative Cooling Circuits for Liquid Rocket Engines," AIAA paper 2006-58219, presented at the Joint Propulsion Conference, Sacramento, California 2006](#)